Published in final edited form as:
Comput Methods Programs Biomed. 2011 May ; 102(2): 219–226. doi:10.1016/j.cmpb.2010.03.008.

Systematic Method to Assess Microvascular Recruitment using Contrast-Enhanced Ultrasound. Application to Insulin-Induced Capillary Recruitment in Subjects with T1DM

Alice Chan, **Boris P. Kovatchev**, **Stacey M. Anderson**, and **Marc D. Breton**
University of Virginia Health System, P.O. 400 888, Charlottesville, VA 22908-4888

Abstract

Contrast-enhanced ultrasound (CEU) is an ultrasound imaging technique used to assess tissue perfusion. Analysis of microvascular recruitment necessitates the definition of a region of interest (ROI) containing exclusively the tissues to be studied. Conventional ROI selection requires examining the images and drawing the ROI by hand, making the analysis of CEU images non-reproducible and analyst-dependent. We have designed a systematic ROI selection method that is both reproducible and analyst-independent. Microvascular blood volume (MBV) assessed in 21 sequences of images was used to correlate the systematic ROI selection method with the conventional method performed by two independent analysts (correlation of 0.88 and 0.87 respectively) and the MBV sample distribution from the systematic method was not significantly different from those obtained from the conventional one. Using the systematic method, we found no significant insulin-induced capillary recruitment in subjects with type 1 diabetes mellitus, which might be related to the observed low glucose uptake during the hyperinsulinemic euglycemic clamp compared to healthy patients.

Keywords

contrast-enhanced ultrasound (CEU); ROI selection; systematic method; microvascular recruitment

1. Introduction

Contrast-enhanced ultrasound (CEU) is a noninvasive technique developed to image myocardial perfusion: inert gas-filled microbubbles are continuously infused into the vascular system and serve as the contrast agent; the microbubbles are then destroyed with high-energy ultrasound, and the rate at which the microbubbles replenish the ultrasound

Author of correspondence: Alice Chan, University of Virginia Health System, P.O. 400 888, Charlottesville, VA 22908-4888, Phone: 646-919-9330, Fax: 434-982-6765, alicechan@virginia.edu.
Alice Chan, Diabetes Technology Center, University of Virginia Health System, P.O. 400 888, Charlottesville, VA 22908-4888, (phone) 646-919-9330, (fax) 434-982-6765, alicechan@virginia.edu
Stacey M. Anderson, M.D., University of Virginia Health System, Department of Internal Medicine, P.O. Box 800466, Charlottesville, VA 22908, Phone: 434-924-5607, SG4C@hscmail.mcc.virginia.edu
Boris P. Kovatchev, Ph.D., Diabetes Technology Center, University of Virginia Health System, P.O. 400 888, Charlottesville, VA 22908-4888, (phone) 434-924-5592, (fax) 434-982-6765, boris@virginia.edu
Marc D. Breton, Ph.D., Diabetes Technology Center, University of Virginia Health System, P.O. 400 888, Charlottesville, VA 22908-4888, (phone) 434-982-6484, (fax) 434-982-6765, mb6nt@virginia.edu

beam reflects the microvascular flow velocity while the concentration of microbubbles when the beam is fully replenished is proportional to the microvascular blood volume (MBV) [1,2,3]. The microbubbles, comparable in size to red blood cells (RBCs), remain entirely within the vascular space and possess similar intravascular rheology to that of RBCs [4,5,6]. It was demonstrated that microbubbles have no significant effects on coronary blood flow and systemic hemodynamics when injected into the circulation [7]. To isolate the tissues to be analyzed from the surrounding tissues, e.g. larger vessels, bones …, a region of interest (ROI) is defined within the space captured by the ultrasound beam. The selection of the ROI requires a trained analyst to go through the ultrasound images and hand-select the region based on his/her expertise. This process is tedious and time consuming, and above all, not reproducible: not two analysts (or even the same analyst doing the analysis twice) will pick the same ROIs and thus potentially not arrive at the same conclusion. Therefore, more systematic ROI selection methods are needed to improve the usability of CEU and make the quantification analyst-independent.

CEU has also been successfully used for measurement of tissue perfusion in the skeletal muscle [8,9,10,11], skin [12], brain [13] and kidney [14]. We apply the proposed method to insulin-mediated changes of blood volume in capillaries of skeletal muscles in subjects with type 1 diabetes mellitus (T1DM). CEU has been used to show that in healthy subjects, insulin-mediated capillary recruitment precedes increases in total blood flow [15,16,17] and is a key part of insulin's action in vivo, accounting for as much as 50% of the insulin-induced increase in glucose uptake [18,9,8,15]. As "insulin-induced alteration in blood flow patterns could be as important as direct signaling of cells by insulin in establishing the rate of glucose utilization in vivo" [19], we examine the effects of insulin on capillary recruitment in T1DM patients as they depend on exogenous insulin supplies to ensure glucose absorption and maintain safe glucose levels.

We propose a method that systematically selects ROIs, insuring consistency in ROI selection in a fast and tractable manner. As point of comparison, two expert analysts were asked to select ROIs on a dataset on which the proposed method was applied as well. Results demonstrated that development of systematic ROI selection can be beneficial to CEU analysis and we applied the method to the analysis of insulin-induced capillary recruitment in T1DM patients.

2. Research design and methods

2.1. Contrast-enhanced ultrasound imaging

Microbubbles are continuously infused in the circulation to provide the contrast medium to the ultrasound imaging technique. When exposed to high-energy ultrasound, the microbubbles are destroyed, resulting in a high-amplitude signal. Ultrasound pulses are gated to an internal timer to allow variable time intervals between pulses. The rationale is to destroy the microbubbles during the first ultrasound pulse and image their reappearance within the muscle vasculature with the second pulse. During an imaging sequence, the interval between these pulses is progressively prolonged to allow more replenishment of the microbubbles in the microcirculation, resulting in an increased signal intensity. Pulsing intervals are usually gated by cardiac cycles (measured by heart beats) so as to keep the blood pressure consistent within the cardiac cycle during the imaging process, and several images are acquired at each pulsing interval (PI) for more robust estimation of the intensity. When the space defined by the beam thickness is completely filled, increasing the pulsing interval does not affect the signal intensity anymore (fig. 1 [A]). The replenishment curve, plot of the mean intensity over a ROI against the pulsing interval, converted into relative time (e.g. milliseconds), can generally be described by an exponential function [3]:

$$y=A(1-e^{-\beta t})+c \quad (1)$$

where y is the ROI mean acoustic intensity in decibels (dB) and t the pulsing interval in milliseconds. The constant c is the acoustic intensity that would be obtained if the pulsing interval was reduced to 0, that is, the intensity reflected by the tissues other than blood vessels, or in other words, reflected by the "background". The parameter A represents the plateau of the background-subtracted intensity and β the rate at which it rises (fig. 1 [B]). As detailed in [3], MBV is estimated by the parameter A.

2.2. Conventional ROI selection

Standard image analysis requires a quantification software such as Q-Lab (Philips Medical Systems) (e.g. [20,11,21,22]). Once a sequence is loaded, the software enables ROI selection for that sequence, computation of the mean signal intensity in the ROI for each image, and estimation of MBV by fitting an exponential function to the replenishment curve. The ROI selection for each sequence has to be done by an expert analyst, who goes through each image of the sequence, and then draws the contour of the ROI by hand on one of the images. The accuracy of the selection to only contain the tissues of interest solely depends on the expertise of the analyst.

Two independent expert analysts were asked to analyze a subset of all the sequences obtained using the conventional method, i.e. by going through all the images of each sequence, and hand-selecting the ROIs. The ROIs were selected to contain capillaries only. MBV was then measured by fitting an exponential function to the replenishment curve (see section 2.1).

2.3. Systematic ROI selection

In order to make the ROI selection analyst-independent and guarantee consistency in the ROI definition across different sequences, we propose a systematic procedure to select ROI, implemented in Matlab (The MathWorks, Inc). In particular, as we focus on insulin-induced capillary recruitment, we present the systematic method for selecting capillaries, and excluding any larger blood vessels from the ROI, such as arteries or veins.

Each sequence of images is loaded in Matlab and converted into a sequence of 2D arrays by means of an open source code developed by Francois Nedelec (EMBL, Heidelberg, Germany). The intensity stored in the TIF files is a [0–255] normalized intensity of the acoustic signal, providing grounds to set a region selection methodology based on pixel intensities applicable to all sequences. The capillary-only ROI selection for each sequence is the following: the whole image is considered as potential ROI to begin with. Because it takes about 2 to 4 heart beats (hb) for the microbubbles to reappear in the capillaries, regions showing stronger signals than a threshold K_1 for any frame taken at a pulsing interval less or equal than 2 hb are discarded. For the intensity reflected by capillaries is limited by the size of the capillaries, regions showing intensity above a threshold K_2 at any pulsing interval are discarded. The resulting region defines the ROI of the sequence (fig. 2). The thresholds were set to match the intensity level above which the analysts would consider a region too bright to contain capillaries only for initial frames and the intensity level above a region would not be included in the ROI regardless of the frame considered for K_1 and K_2 respectively. The values were set to $K_1 = 50$ and $K_2 = 150$.

Although pulsing interval is gated by cardiac cycles, the TIF file only stores the pulsing interval converted into relative time (in milliseconds). In order to retrieve the information in

heart beats, we developed an algorithm that proceeds in two phases. The first phase consists in determining the steps of the sequence of pulsing intervals. As mentioned earlier, several frames are usually taken at the same pulsing interval before the pulsing interval is increased, so in other words, the sequence of pulsing intervals is a stepwise increasing sequence. However, due to small variation of the heart rate, frames taken at the same number of heart beats do not show the exact same relative time. In order to reconstruct the steps of the sequence, or equivalently, the "transition" frames, i.e. the frames before each step, we proceed as follows:

1. Consider the sequence of frames $F = \{f_1, f_2, \ldots, f_n\}$ with corresponding sequence of relative times $T = \{t_1, t_2, \ldots, t_n\}$ and normalized differences

$$D=\{d_1, d_2, \ldots, d_{n-1}, d_n\}=\left\{\frac{t_2-t_1}{t_1}, \frac{t_3-t_2}{t_2}, \ldots, \frac{t_n-t_{n-1}}{t_{n-1}}, 0\right\}$$

   Using a sliding window of size m, compute the standard deviation of the subsets D_i's of normalized differences and denote s_0 the smallest standard deviation obtained.

$$D_i=\{d_i, d_{i+1}, \ldots, d_{i+m-1}\} \subset D$$
$$s_0=\min_{D_i}\left\{s_i : s_i=\sqrt{\mathrm{var}(D_i)}\right\}$$

   Let F_T be the set of potential transition frames. A frame f_i is in F_T if its corresponding normalized difference is greater than s_0.

$$d_i \geq s_0 \Rightarrow f_i \in F_T$$

2. More than one frame was taken at each pulsing interval, so for each group of consecutive potential transition frames, keep in F_T the frame with higher normalized difference and take all the other ones out of the set.

$$(d_i, \ldots, d_{i+k}, \in F_T \text{ and } d_{i_0}=\max\{d_i, \ldots, d_{i+k}\}) \Rightarrow d_{i,i\neq i_0} \notin F_T$$

   Denote τ the strictly increasing map that defines the frames in F_T: $F_T = \{f_{\tau(1)}, f_{\tau(2)}, \ldots, f_{\tau(p)}\}$, with p the size of the set F_T.

3. Let $S_{\tau(i)}$ the step defined by $f_{\tau(i)}$ in F_T, i.e. including the frames $f_{\tau(i)+1}, \ldots, f_{\tau(i+1)}$. Define $t_{S_{\tau(i)}}$ the relative time of a step $S_{\tau(i)}$ as the median of the relative times of the frames contained in it and merge the steps with decreasing relative time with the previous one.

$$t_{S_{\tau(i+1)}} < t_{S_{\tau(i)}} \Rightarrow S_{\tau(i+1)}=S_{\tau(i)}$$

4. If imaging was continued beyond the replenishment curve, that is, at the same last pulsing interval to capture changes in MBV (intensity reflected when the beam space is fully replenished), ensure that only the last step $S_{\tau(p)}$ can be of size greater

than n_{max}. Otherwise, collapse that step with the following one. The parameter n_{max} is the maximum possible length for all the steps but the last one.

$$\tau(i+1) - \tau(i) \geq n_{\max} \Rightarrow S_{\tau(i+1)} = S_{\tau(i)}$$

where $\tau(0) = 0$.

Denote v the map defining the transition frames resulting from the set of steps obtained: $F_T = \{fv_{(1)}, fv_{(2)}, \ldots, fv_{(q)}\}$, with q the size of the set F_T, and the corresponding steps $Sv_{(i)}$ and relative times $t_{Sv(i)}$. After identification of the steps of the sequence of frames, the second phase is to determine $h_{Sv(i)}$ the heart beat of the steps. Based on the relative times $t_{Sv(i)}$ and the knowledge of the heart beat of the last pulsing interval used, the full sequence can be estimated as detailed:

1. Estimate HR the heart rate using the last pulsing interval as the ratio of number of heart beats over corresponding relative time.

$$\mathrm{HR} = \frac{h_{S_{v(p)}}}{t_{S_{v(p)}}}$$

2. Based on the estimated heart rate, estimate the pulsing interval in heart beats of the preceding frame as ratio of the heart rate over the relative time of that frame, rounded to the closest integer. Update the heart rate estimate as weighted mean of number of heart beats over corresponding relative time of the computed frames. The weights are taken to fall exponentially from the last estimate with rate α. The larger α, the more weight is given to recent estimates over older ones.

$$h_{S_{v(i)}} = \lfloor \mathrm{HR} \times t_{S_{v(i)}} \rfloor$$
$$\mathrm{HR} = \sum_{k=p}^{i} w_{k,i} \frac{h_{S_{v(k)}}}{t_{S_{v(k)}}}$$
$$w_{k,i} = \frac{e^{-\alpha(k-i)}}{\sum_{k=p}^{i} e^{-\alpha(k-i)}}$$

3. Repeat 2. till the first frame of the sequence.

For the sequences of our study, a window size m of approximately one sixth of the sequence length proved to be appropriate. The window size was thus set to $m = 20$ for the “basal” sequences (long sequences containing about 120 images each) and to $m = 5$ for the “30 min” ones (short sequences containing about 30 images each, see section 2.4). The algorithm was robust to the window size m when set to values up to a forth of the sequence length. Approximately five frames per pulsing interval were taken for low pulsing interval (PI = 1 and 2) and about three for the other ones. In any case, the number of frames per pulsing interval did not exceed 8 so the parameter n_{max} was set to $n_{max} = 8$. Finally, the parameter α was set to $\alpha = 0.001$ such that the current estimate of the heart rate was heavily based on the past estimates. The conversion of the pulsing interval from relative time to heart beats remained unchanged for values of α as low as 0.0001. Thus, the pulsing intervals in heart beats were retrieved for each sequence of images. The ROI mean pixel intensity was then computed, converted back to acoustic intensity using a scale stored in the TIF file and plotted against the pulsing interval to obtain the replenishment curve, thus allowing for the determination of MBV.

2.4. Hyperinsulinemic euglycemic clamp

The study was approved by the University of Virginia Internal Review Board and performed at the University of Virginia General Clinical Research Center (GCRC). All subjects gave informed consent. Twenty-six hyperinsulinemic euglycemic clamp studies were performed on 17 patients with T1DM (table 1). The clamps performed on the same subject were done at least six months apart from each other. Long-acting insulin was discontinued 60 hours prior to the clamp procedure and intermediate acting insulin was discontinued 36 hours prior to the clamp procedure. Only short or rapid-acting insulin was allowed on the day of the admission. Subjects were admitted to the University of Virginia GCRC on the evening prior to study. At 21:30, an overnight insulin infusion consisting of regular insulin (Novolin R, Novo Nordisk) in 0.9% saline at a concentration of 1:1 was titrated to control the subjects' blood glucose overnight between 100 and 150 mg/dL by sampling YSI plasma glucose every 30 min and adjusting the rate of insulin infusion as needed. This was discontinued at 08:30 the following morning at the initiation of the clamp procedure.

At time 0 of the clamp, an insulin infusion was started via a Harvard pump by a 20 mU/kg priming over 10 minutes followed by a constant 1 mU/min/kg infusion maintained for the next 120 min as described by [23]. Blood glucose was clamped at basal levels via a variable-rate infusion of 20% dextrose. Blood samples for total insulin and plasma glucose levels were taken throughout the study at intervals of at most ten minutes.

CEU was performed with a SONOS 7500 ultrasound system (Philips Medical Systems, Bothell, WA) and a S3 probe. Imaging was performed in the forearm with an ultrasound transmit frequency of 1.3 MHz and receive frequency of 3.6 MHz. A 3 mL suspension of octafluoropropane gas-filled lipid microbubbles Definity (Bristol-Myers Squibb Medical Imaging, North Billerica, MA) diluted in 57 mL saline and infused at a rate of 1.5 mL/min was used as the contrast medium. CEU imaging was performed at time 0 and 30 min after the start of the clamp, yielding a total of 52 sequences of images. Images were obtained at increasing pulsing interval, from 1 to 20 cardiac cycles, with at least 3 images acquired at each pulsing interval. The sequences of ultrasound images were digitalized and stored as TIF files for offline analysis. Capillary recruitment was assessed by MBV and the acquisition of a sequence of images necessary to estimate MBV takes approximately 5 minutes. Therefore, the first sequence captures capillary recruitment at basal rate of plasma insulin while the second sequence captures capillary recruitment under hyperphysiological insulin concentration levels. These two sequences will be denoted as the "basal" and the "30 min" sequence respectively.

2.5. Statistical analysis

One of the clamps was discarded from the analysis as a premature disappearance of the microbubbles in the solution made the sequence of images unusable, thus leaving 25 clamps and a total of 50 sequences of images to be analyzed. Because selecting ROIs through the conventional method is time-consuming and tedious, the systematic ROI selection method was compared to the conventional method on a subset of the sequences. The subset of sequences was determined as half the total number of sequences at a time when eight sequences were not available. Thus, twenty-one out of the 50 sequences were analyzed by two expert analysts using the conventional method. The resulting MBV were then compared to those obtained with the systematic method by means of correlation and linear regression. The sampling distributions of the MBVs were compared using Fisher's exact tests due to the small sample size. For all the tests, statistical significance was declared at 0.05.

3. Results

3.1. ROI selection methods comparison

For the subset of 21 sequences of images, MBV was calculated using the systematic and conventional ROI selection methods. The ROIs obtained from the systematic method and the two analysts are represented in fig. 3 for one sequence.

MBV obtained from the systematic method was compared to MBV obtained from ROIs selected from analysts 1 and 2. The linear fit between MBV obtained from the systematic method and from analyst 1 was statistically significant ($p < 0.001$). The estimates of the slope and intercept were (expressed as mean ± standard error) 1.074±0.130 and 0.289±0.553 respectively. The linear fit between MBV obtained from the systematic method and from analyst 2 was also statistically significant ($p < 0.001$). The estimates of the slope and intercept were 0.988 ± 0.130 and 1.139 ± 0.552 respectively. The correlations between MBV derived from the systematic method and from ROIs conventionally selected were very good, 0.88 and 0.87 for analyst 1 and 2 respectively, with corresponding p-values for the t-test of correlation being different from 0 equal to 0.01 and 0.03 respectively (see fig. 4 and 5).

The MBV values obtained within the conventional method were coherent: the correlation between ROIs obtained by the two analysts was 0.93 ($p < 0.001$).

Sample distributions of MBV were constructed using three bins: 0 to 3 dB, 3 to 6 dB and greater than 6 dB; results are shown in fi. 6. Fisher's exact tests were performed between the sample distribution of MBV obtained from the systematic method and from analyst 1, and between the sample distribution of MBV obtained from the systematic method and from analyst 2. As shown in table 2, none of the tests were significant, meaning that the hypothesis that the MBV values from the systematic method come from the same distribution as MBVs from analyst 1 or 2 cannot be rejected. The Fisher's test between MBVs from analysts 1 and 2 confirms the coherence within the conventional method. These results provide ground to apply the systematic ROI selection method to measure microvascular recruitment with CEU.

4. Discussion

4.1. Systematic ROI selection method

We developed a systematic method to select ROI in CEU imaging analysis. The presented systematic ROI selection method was compared to ROIs obtained from the conventional method, that is, from analysts hand selecting ROIs for each sequence. Two expert analysts were asked to perform the task on a subset of our sequences and the MBV values obtained were compared with each other. Very good correlations were obtained between the systematic ROI selection method and ROIs selected from both analysts and the linear fits suggested that a 1:1 relation between the methods could not be rejected at a 0.05 level of significance. These results indicate that systematic ROI selection in CEU analysis reproduce state of the art methods, while ensuring speed and reproducibility.

Such systematic methods will allow the analysis to be analyst-independent. The conventional way to select ROIs requires the analyst to select ROIs for each sequence by hand, implying that conclusions drawn from one analyst might be different from those reached by another analyst as estimates of tissue perfusion follow the ROI selection. Systematic methods enable ROIs to be defined consistently across sequences of images and bypass the subjectivity of analyst-defined ROIs. Furthermore, systematic methods are reproducible, that is, the same sequence of images will always yield the same ROI and thus

the same microvascular perfusion assessment. Without systematic methods, the same sequence analyzed by the same person could yield diferent results.

Moreover, the conventional ROI selection method is time consuming as it requires the analyst to go through the whole sequence and then draw the region “by hand”. On the contrary, the ROI is selected within a couple of seconds by the systematic method. The implementation of a systematic method to select ROI speeds up the analysis of CEU images, a feature of particular importance in low-energy ultrasound pulse real-time assessment of tissue perfusion [13]. While high-energy ultrasound destroys the microbubbles, low-energy pulses make them oscillate nonlinearly with minimal destruction, allowing for real-time imaging.

Additionally, the systematic method enables ROIs to be composed of several non-adjacent regions and hence accounts for more capillaries compared to a sole continuous ROI allowed by existing softwares. As the surface of the ROI is increased, more of the tissues are taken into account thus providing more robust assessment of microvascular recruitment.

Although we detailed a procedure to define ROI containing capillaries only, based on the microbubble reapparition time and intensity level of the emitted signal in capillaries versus larger blood vessels, the procedure can be adapted to other types of tissues (kidney, heart, brain …) or to include constraints specific to particular sets of images.

4.2. Insulin-induced capillary recruitment

We apply our method to the analysis of insulin-induced capillary recruitment in T1DM patients. The ROI mean intensity was calculated for both the “basal” and “30 min” sequences of each clamp using the systematic method. The replenishment curves were then fitted to all the sequence and the parameters of eq.(1) were estimated. The maximum intensity value is reached at steady state and is equal to the plateau A. Let us denote t_α the time at which the intensity has reached α% of A, which can be derived from eq.(1) and expressed in terms of the parameters as: $t_\alpha = \frac{1}{\beta}\log\left(\frac{A}{(1-\alpha/100)(A+c)}\right)$. In particular, the time to reach 95% of the maximum intensity is $t_{95} = \frac{1}{\beta}\log\left(\frac{A}{0.05(A+c)}\right)$. It is also known that it takes about 10 to 15 seconds for the blood to flow over 1 cm in capillaries and since the length of the probe is 1.2 cm, it would take on average $t_{avg} = 15 \times 1.2$ seconds for the microbubbles to fill the whole space covered by the probe and thus the same amount of time for the intensity to plateau at its maximum value. Values of t_{95} exceeding $3 \times t_{avg}$ were deemed unrealistic and the parameters α, β and c of sequences for which $t_{95} \geq 3 \times t_{avg}$ thus considered not reliable to assess microvascular recruitment; such sequences were removed from the analysis. In total, eight of the 25 clamps were removed, leaving 17 clamps for the analysis.

The “basal” and “30 min” sequences of images yielded measures of MBV at basal rate of plasma insulin and at hyperphysiological insulin concentration levels respectively, which we denote MBV_{basal} and MBV_{30min}. The relative change in MBV, in percentage, from the basal state to the hyperinsulinemic state, was defined as:

$$\Delta MBV = \frac{MBV_{30\,min} - MBV_{basal}}{MBV_{basal}} \times 100$$

The mean relative change in MBV was 0.6% and the standard deviation 33.8%. The paired t-test indicated that the null hypothesis of no relative change in MBV could not be rejected at a 0.05 level of significance. The effect of insulin on capillary recruitment observed in healthy patients could not be confirmed in T1DM patients with our dataset. As detailed in

[23], the variable glucose infusion rate averaged during the steady state of the hyperinsulinemic euglycemic clamp, denoted M-value and measured in mg/min/kg, is a measure of the whole-body glucose uptake flux. The M-value of each clamp was computed over the last 30 min of the clamp when steady state was reached. The M-values ranged from 1.75 to 6.86 mg/min/kg with mean value of 4.31. These values are below the average 7 mg/min/kg measured in healthy subjects under a euglycemic hyperinsulinemic clamp, but do agree with the average 4.3±0.6 mg/min/kg obtained for patients with T1DM [24]. This difference in glucose uptake during a hyperinsulinemic euglycemic clamp in T1DM versus healthy patients might be related to the action of insulin on the microvasculature. While the link between increased capillary recruitment and glucose utilization was demonstrated in healthy patients, further analysis is needed to investigate how capillary recruitment relates to glucose absorption in T1DM and how it might affect direct signalling to tissues.

Supplementary Material

Refer to Web version on PubMed Central for supplementary material.

Acknowledgments

The authors would like to thank Eugene Barrett, M.D., Ph.D. and Zhenqi Liu, M.D. (University of Virginia) for the time they took to analyze the images, as well as Francois Nedelec (EMBL, Heidelberg, Germany) for providing the Matlab code that reads TIF files.

This study is supported by the NIH/NIDDK RO1 DK 51562 grant and the University of Virginia General Clinical Research Center M01 RR 000847 grant.

References

1. Wei K, Kaul S. Recent advances in myocardial contrast echocardiography. Current Opinion in Cardiology. 1997; 12(6):539–46. [PubMed: 9429825]
2. Wei K, Skyba D, Firschke C, Jayaweera A, Lindner J, Kaul S. Interactions between microbubbles and ultrasound: in vitro and in vivo observations. Journal of the American College of Cardiology. 1997; 29(5):1081–8. [PubMed: 9120163]
3. Wei K, Jayaweera AR, Firoozan S, Linka A, Skyba DM, Kaul S. Quantification of myocardial blood flow with ultrasound-induced destruction of microbubbles administered as a constant venous infusion. Circulation. 1998; 97:473–483. [PubMed: 9490243]
4. Jayaweera A, Edwards N, Glasheen W, Villanueva F, Abbott R, Kaul S. In vivo myocardial kinetics of air-filled albumin microbubbles during myocardial contrast echocardiography. Comparison with radio-labeled red blood cells. Circ Res. 1994; 74(6):1157–1165. [PubMed: 8187282]
5. Lindner J, Song J, Jayaweera A, Sklenar J, Kaul S. Microvascular rheology of definity microbubbles after intra-arterial and intravenous administration. Journal of the American Society of Echocardiography. 2002; 15(5):396–403. [PubMed: 12019422]
6. Lepper W, Belcik T, Wei K, Lindner JR, Sklenar J, Kaul S. Myocardial Contrast Echocardiography. Circulation. 2004; 109(25):3132–3135.10.1161/01.CIR.0000132613.53542.E9 [PubMed: 15226230]
7. Keller M, Glasheen W, Teja K, Gear A, Kaul S. Myocardial contrast echocardiography without significant hemodynamic effects or reactive hyperemia: a major advantage in the imaging of regional myocardial perfusion. J Am Coll Cardiol. 1988; 12(4):1039–1047. [PubMed: 3417978]
8. Rattigan S, Clark M, Barrett E. Hemodynamic actions of insulin in rat skeletal muscle: Evidence for capillary recruitment. Diabetes. 1997; 46:1381–1388. [PubMed: 9287035]
9. Coggins M, Lindner J, Rattigan S, Jahn L, Fasy E, Kaul S, Barrett E. Physiologic hyperinsulinemia enhances human skeletal muscle perfusion by capillary recruitment. Diabetes. 2001; 50:2682–2690. [PubMed: 11723050]
10. Dawson D, Vincent MA, Barrett EJ, Kaul S, Clark A, Leong-Poi H, Lindner JR. Vascular recruitment in skeletal muscle during exercise and hyperinsulinemia assessed by contrast

ultrasound. Am J Physiol Endocrinol Metab. 2002; 282(3):E714–720.10.1152/ajpendo.00373.2001 [PubMed: 11832377]

11. Ross RM, Downey K, Newman JM, Richards SM, Clark MG, Rattigan S. Contrast-enhanced ultrasound measurement of microvascular perfusion relevant to nutrient and hormone delivery in skeletal muscle: A model study in vitro. Microvascular Research. 2008; 75(3):323–329. [PubMed: 18207201]
12. Christiansen JP, Leong-Poi H, Amiss LR, Drake DB, Kaul S, Lindner JR. Skin perfusion assessed by contrast ultrasound predicts tissue survival in a free flap model. Ultrasound in Medicine and Biology. 2002; 28(3):315–320.10.1016/S0301-5629(01)00523-3 [PubMed: 11978411]
13. Rim S, Leong-Poi H, Lindner J, Couture D, Ellegala D, Mason H, Durieux M, Kassel N, Kaul S. Quantification of cerebral perfusion with “real-time” contrast-enhanced ultrasound. Circulation. 2001; 104:2582–2587. [PubMed: 11714654]
14. Wei K, Le E, Bin JP, Coggins M, Thorpe J, Kaul S. Quantification of renal blood flow with contrast-enhanced ultrasound. J Am Coll Cardiol. 2001; 37(4):1135–1140. [PubMed: 11263620]
15. Vincent M, Dawson D, Clark A, Lindner J, Rattigan S, Clark M, Barrett E. Skeletal muscle microvascular recruitment by physiological hyperinsulinemia precedes increases in total blood flow. Diabetes. 2002; 51(1):42–48. [PubMed: 11756321]
16. Vincent M, Clerk L, Lindner J, Klibanov A, Clark M, Rattigan S, Barrett E. Microvascular recruitment is an early, direct insulin effect that regulates skeletal muscle glucose uptake in vivo. Diabetes. 2004; 53:1418–1423. [PubMed: 15161743]
17. Zhang L, Vincent M, Richards S, Clerk L, Rattigan S, Clark M, Barrett E. Insulin sensitivity of muscle capillary recruitment in vivo. Diabetes. 2004; 53:447–453. [PubMed: 14747297]
18. Clerk L, Vincent M, Lindner J, Clark M, Rattigan S, Barrett E. The vasodilatory actions of insulin on resistance and terminal arterioles and their impact on muscle glucose uptake. Diabetes Metab Res Rev. 2004; 20:3–12. [PubMed: 14737741]
19. Bergman R. Editorial: Insulin action and distribution of tissue blood flow. J Clin Endocrinol Metab. 2003; 88:4556–4558. [PubMed: 14557421]
20. Eggleston EM, Jahn LA, Barrett EJ. Hyperinsulinemia rapidly increases human muscle microvascular perfusion but fails to increase muscle insulin clearance: Evidence that a saturable process mediates muscle insulin uptake. Diabetes. 2007; 56(12):2958–2963. [PubMed: 17720897]
21. Toledo E, Lodato J, DeCara J, Collins K, Bednarz J, Lang R, Mor-Avi V. Echocardiographic detection of stfess-induced myocardial ischemia using quantitative analysis of contrast-enhanced parametric perfusion images. Computers in Cardiology. 2004:233–236.
22. Kalantarinia K, Okusa MD. Ultrasound contrast agents in the study of kidney function in health and disease. Drug Discovery Today: Disease Mechanisms. 2007; 4(3):153–158. [PubMed: 19112526]
23. DeFronzo R, Tobin J, Andres R. Glucose clamp technique: a method for quantifying insulin secretion and resistance. Am J Physiol Gastroin-test Liver Physiol. 1979; 237(3):G214–223.
24. Roden, M. Clinical Diabetes Research: Methods and Techniques. 1. Wiley-Interscience; 2007.

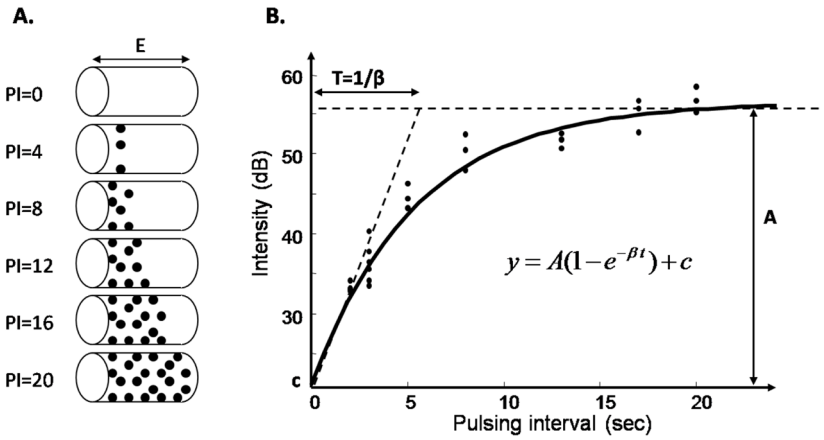

Figure 1.

Replenishment curve. A. The thickness of the ultrasound beam is represented as E. At PI = 0, all the microbubbles are destroyed by the first ultrasound pulse of ultrasound. As the pulsing interval is increased, more microbubbles reappear. B. The mean intensity within the ROI is plotted versus the pulsing interval. The parameter *A* is a measure of MBV.

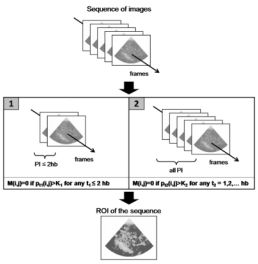

Figure 2.

Systematic ROI selection. Let M represents the ROI and $p_t(i, j)$ the pixel intensity at position (i, j) of a frame taken at t heart beats. Initially, all pixels are considered in the ROI, i.e. $M(i, j) = 1$ for all pixels. [1] Set $M(i, j) = 0$ if there exists a frame taken at PI ≤2 hb which intensity at (i, j) exceeds K_1. [2] Set $M(i, j) = 0$ if among all frames, the intensity at (i, j) exceeds K_2 at least once. The resulting M is the ROI.

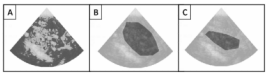

Figure 3.
Systematic and conventional ROI selection. The selected ROI is represented in dark for one sequence of CEU images. A. Systematic ROI selection methodology. B. ROI selection from analyst 1. C. ROI selection from analyst 2.

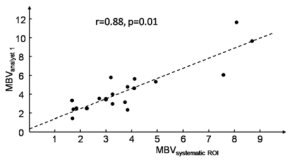

Figure 4.
Relation between MBV obtained from the systematic ROI selection method and from ROI selected from analyst 1.

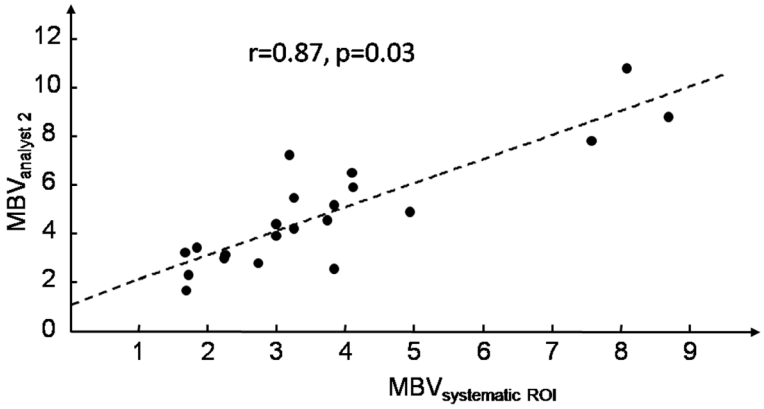

Figure 5.
Relation between MBV obtained from the systematic ROI selection method and from ROI selected from analyst 2.

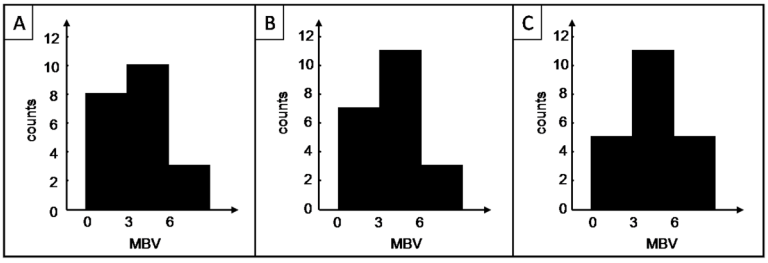

Figure 6.
Histograms of MBV obtained with different ROI selection method. A. From the systematic ROI selection method. B. From analyst 1. C. From analyst 2.

Table 1

Demographic characteristics of the study group

	Mean ± SD
M/F	13/4
Age (years)	38.3 ± 12.6
Weight (kg)	81.3 ± 13.7
HbA1c (%)	7.7 ± 1.6
Years since diagnosed T1DM	20.3 ± 11.8

Table 2

Fisher's exact tests' p-values comparing MBV resulting from the systematic ROI selection and selection by analysts 1 and 2

	Analyst 1	Analyst 2
Systematic ROI selection	1	0.51
Analyst 1		0.66